Supplemental Table 1: Primer Sequences

Application	Gene	5' – 3' FWD	5' – 3' REV
qPCR	mCyclo	ATGGTCAACCCCACCGTGT	TTCTGCTGTCTTTGGAACTTTGTC
	mEtv1	GAAGGGTCCCAGGCAGTTCT	AACTTCTCCGGGACCACACA
	mMMP3	TGGAACAGTCTTGGCTCATGCCTA	TGGGTACATCAGAGCTTCAGCCTT
	mMMP7	AACACTCTAGGTCATGCCTTCGCA	AGACCCAGAGAGTGGCCAAATTCA
	mMMP9	TGAACAAGGTGGACCATGAGGTGA	TAGAGACTTGCACTGCACGGTTGA
	mCdh1	TCAAGCTCGCGGATAACCAGAACA	ATTCCCGCCTTCATGCAGTTGTTG
	mCdh2	ATGGCCTTTCAAACACAGCCACAG	ACAATGACGTCCACCCTGTTCTCA
	mSlug	CCACACATTGCCTTGTGTCTGCAA	TGTGCCCTCAGGTTTGATCTGTCT
	mSnail	ACACTGGTGAGAAGCCATTCTCCT	TCTTCACATCCGAGTGGGTTTGGA
	mTwist	AGCTGAGCAAGATTCAGACCCTCA	TGCAGCTTGCCATCTTGGAGT
	mVimentin	AAGCACCCTGCAGTCATTCAGA	GCAAGGATTCCACTTTCCGTTC
	mZeb1	TGAGCACACAGGTAAGAGGCC	GGCTTTTCCCCAGAGTGCA
	mZeb2	TGATAGCCTTGCAAACCCTCTGGA	TCCTTCATTTCTTCTGGACCGGCT
	mCol1a1	GCTTGAAGACCTATGTGGGTATAA	GGTGGAGAAAGGAGCAGAAA
	mCol3a1	CCTGGTGGAAAGGGTGAAAT	CGTGTTCCGGGTATACCATTAG
	mFAP	AGGAGGTTAGGCTCGGTATT	CCGGCAATGAACAGGTGATA
Cloning	mEtv1 (Age1, MluI)	ACTGAACCGGTAGCAGCATGGATGGATTTTATGACCAGCA	AATCGACGCGTTTAGTACACGTATCCTTCGTTGTAGGGGTG
	mHas2 (Age1, MluI)	ACT GAA CCG GTA GCA GCA TGC ATT GTG AGA GGT TTC TAT GTG TCC TG	AAT CGA CGC GTT CAT ACA TCA AGC ACC ATG TCA TAC TGT TGT C
	FLAG-mEtv1 (Age1, Mlu1) into pTripz	ACTGAACCGGTGCCACCATG GAT TAC AAG GATGACGACGATAAGGATGGATTTTATGACC AGCAAGTGCC	AATCGACGCGTTTAGTACACGTATCCTTCGTTGTAGGGGTG
	Sparc-pGL3basic-luc (Mlu1,Xho1)	ACTGACGCGTGTGTCTGGGTAGCACACAGC CTA	ACTGCTCGAGCATGATGCTGGGAACTCTCGGCA
	Has2-pGL3basic-luc (Mlu1, Xho1)	ACTGACGCGTGGGGAGACGTTGACATTTGC CT	ACTGCTCGAGTTTGCTCCAATCCCCTTCCCTC
Site Directed Mutagenesis	Has2 wt	ACTGACGCGTGAGCTGGGAGGAAGAAAG GGTTAAC	ACTGCTCGAGTTTGCTCCAATCCCCTTCCCTC
	Has2 mut	ACTGACGCGTGAGCTGGGAGACAGAAAG GGTTAAC	ACTGCTCGAGTTTGCTCCAATCCCCTTCCCTC

SUPPLEMENTAL FIGURE LEGENDS

Supplemental Figure 1:

(A) Immunohistochemistry for Etv1 in human low- and high- grade PanIN from a Tissue Microarray (TMA). Etv1 is expressed in 88% (15/17) of the low-grade PanIN and 100% (5/5) of the high-grade PanIN with similar staining grades in both cohorts. Staining is predominantly nuclear with occasional cytoplasmic staining also seen. **(B)** Immunohistochemistry for Etv1 in matched human primary PDAC and paired metastasis from a rapid autopsy cohort TMA. Etv1 is expressed in 88%(14/16) of the examined primary and in 94% (15/16) matched metastatic lesions with a similar distribution of staining intensity. Staining is predominantly nuclear with occasional cytoplasmic staining also seen. **(C)** Immunohistochemistry for Etv1 in the tumor areas and matched tumor associated stromal areas of human PDAC. Etv1 is expressed in both compartments in all examined tumors (7/7). **(D)** Immunohistochemistry for Etv1 in matched mouse primary PDAC (KPfC) and paired liver metastasis. Etv1 is expressed in 100% (5/5) of the examined primary and in 80% (4/5) matched liver metastatic lesions. **(E)** Etv1 expression in normal human pancreas vs. PDAC. Data from www.oncomine.org. Data from 39 samples analyzed using the Human Genome U133 Plus 2.0 Array (37). A 5.12 fold increase in Etv1 expression was found in human PDAC in comparison to matched normal controls ($p<6.96x10^{-16}$).

Supplemental Figure 2:

(A) Quantitative PCR for Etv1 in wild type, control and lentivirally transduced mEtv1 over-expressing cell lines: **(Left)** Stepwise increase in mEtv1 gene

expression by qPCR in comparing wild type pancreatic ductal cells (PDC) with parental cell lines from KC (PanIN) and KPfC (PDAC) animals. There is a 15-fold increase in Etv1 between PDC and PanIN, and a 184-fold increase in Etv1 between PDC and PDAC cell lines. **(Right)** A consistent Etv1-overexpression of 6-9 fold after lentiviral transduction was seen across cell lines as compared to respective controls. *p<0.001 **(B)** Western blot for FLAG-M1 in KPfC, KPfC mEtv1, KPfC Sparc$^{-/-}$ Control, KPfC Sparc$^{-/-}$ mEtv1, KPfCY Control, and KPfCY mEtv1 cell lines used for orthotopic xenograft experiments. Respective parental cell lines were lentivirally transduced with Etv1-FLAG or empty vector (Control). β-actin served as loading control. **(C)** Treatment of KPfC PDAC-cells with the MEK-inhibitor U0126 resulted a significantly decreased expression of Etv1 compared to DMSO control. *p<0.001.

Supplemental Figure 3:

(A) Ki67 positive cells per high power field in KPfCY Control and KPfCY mEtv1 tumors. There is no significant difference seen. **(B)** TUNEL positive cells per high power field of KPfCY Control and KPfCY mEtv1 tumors. There is no significant difference seen. **(C)** Growth curves of KPfC Control and KPfC mEtv1 cells *in vitro*. WST-1 assay demonstrates an increase in proliferation between KPfC Control and KPfC mEtv1 cells, with control cells proliferating at a slightly higher rate. **(D)** Grading of Ascites in orthotopic transplantation experiments with KPfCY Control and KPfCY mEtv1 tumors. Mice with mEtv1 overexpressing tumors displayed significantly more frequent and higher-grade ascites. **(E)** Quantification of metastatic events in the lungs of animals

undergoing orthotopic transplantation with KPfCY control and KPfCY Etv1. There were significantly more frequent lung metastasis in the Etv1-overexpressing animals in comparison to their controls. All metastatic events seen in the lungs were isolated tumor cells. **(F)** Matched H&E and Immunofluorescence staining for YFP of a representative lung metastasis from a KPfCY mEtv1 xenograft. YFP positive cells from a KPfCY Etv1 tumor have formed a lung metastasis.

Supplemental Figure 4:

(A) Schematic diagram of the Sparc promoter. Green boxes indicate predicted Etv1 binding sites. The promoter fragment upstream of the 5' untranslated region was subcloned into the pGL3 Vector for Luciferase reporter analysis. **(B)** KPfCY mice (n=3) were sacrificed and primary tumors were first sorted by FACS for YFP+ fraction. The YFP+ fraction was then sorted into ECAD+ and ECAD- fractions and RNA isolated. Quantitative PCR demonstrates significantly increased Etv1 and Sparc in the YFP+/Ecad- fraction of 2/3 and 3/3 of these mice, respectively. **(C)** Histology of tumors used for the isolation of YFP+, ECad+/ECad- cell fractions in (B). **(D)** Quantitative PCR for EMT-related genes in KC control and KC mEtv1 cells. KC mEtv1 cells display a significant upregulation in classical regulators of EMT as well as matrix metalloproteases. **(E)** Invasion assay of KC control and KC mEtv1 cells using BD BioCoat™Matrigel Invasion Chambers (8µm Pore size). The invasive capacity of KC mEtv1 cells is significantly increased compared to KC control. **(F)** Knockdown of Etv1 by siRNA leads to a significant downregulation of

Zeb1 in KPfC-cells. The invasive capacity of KPfC-cells is significantly reduced by knockdown of Etv1.

Supplemental Figure 5:

(A) TGF-β-induced EMT in KC cells. Expression of Etv1 is significantly increased with induction of EMT in parallel with *Snail, Zeb1, Zeb2, N-cad*, followed by a decrease in Etv1 and these markers with withdrawal of TGF-β. **(B)** Loss of Sparc abrogates the increased expression of the EMT-markers *Snail, Zeb1* and *Zeb2* mediated by Etv1 in KPfC-cells. **(C)** Immunofluorescence staining for dTom (green) and *Sparc* (red) and E-cadherin (white, lower panel) in KPfC control, KPfC mEtv1 and KPfC Sparc$^{-/-}$ mEtv1 pancreatic orthotopic xenograft primary tumors. Co-localization of dTom and Sparc is present in the KPfC mEtv1 tumors (arrows indicating cells colocalizing), very low in the KPfC control (arrows indicating lack of colocalization) and absent KPfC Sparc$^{-/-}$ Etv1 tumors (arrows indicating lack of colocalization). KPfC mEtv1 xenografts that show co-localization of dTom and *Sparc* are negative for E-cadherin. Host-derived *Sparc* is detected in the KPfC Sparc$^{-/-}$ mEtv1 tumors in the dTom negative tumor associated stroma. **(D)** Quantification of frequency and grade of ascites in KPfC Control, KPfC mEtv1, KPfC Sparc$^{-/-}$ mEtv1 Orthotopic Transplantation Experiment. The increased frequency and grade of ascites observed with KPfC mEtv1 overexpressing xenografts is abrogated by the loss of *Sparc.*

Supplemental Figure 6:

(A) Immunofluorescence staining for YFP (green) and αSMA (red) in KPfCY control and KPfCY mEtv1 tumors. Automated semi-quantitation is shown adjacent. Etv1 overexpressing tumors do not display increased α-SMA expression. **(B)** Number of GFAP-positive cells per high power field in KPfCY control and KPfCY mEtv1 tumors. No significant difference between KPfCY control and KPfCY mEtv1 tumors was observed. **(C)** Immunofluorescence staining for YFP (green) and lysyl-oxidase (LOX) (red) in KPfCY control and KPfCY mEtv1 tumors. Etv1 overexpressing tumors do not show increased expression of lysyl-oxidase. **(D)** Immuno-fluorescence staining for YFP (green) and Collagen I (red) in KPfCY control and KPfCY mEtv1 tumors. Etv1 overexpressing tumors do not show increased expression of Collagen I. **(E)** Quantitative PCR for Collagen I, III, and FAP in KPfCY Control and KPfCY mEtv1 cell lines shows no significant difference.

Supplemental Figure 7:

(A) Left Panel: Expression of Has2 in KPfC - and KPfC Sparc-/- -cells (left panel). There was no significant difference in Has2 between these two cell lines. **Right Panel:** Expression of Sparc in KPfC and KPfC-cells overexpressing Has2. KPfC mHas2 cells had a 4.7 fold increase in Has2 in comparison to respective parental control (data not shown). There was no significant difference in Has2 between these two cell lines. **(B+C)** Staining for hyaluronic acid with the molecular probe HTI601 in KPfC control, KPfC mEtv1 and KPfC $Sparc^{-/-}$ mEtv1 tumors and quantification. KPfC mEtv1 xenografts display significantly larger hyaluronic acid positive areas than KPfC control, similar to findings with KPfCY control and KPfCY mEtv1. The increase in

hyaluronic acid with Etv1 overexpression is completely abrogated by the loss of *Sparc.* **(D)** Correlation of tumor volume and hyaluronic acid positive area in KPfC Control (green dots), KPfC mEtv1 (red dots), and KPfC Sparc$^{-/-}$ mEtv1 (yellow dots).

SUPPLEMENTAL EXPERIMENTAL PROCEDURES

Sorting and Isolation of Ecad+ and Ecad- Fractions from KPfCY Mice

KPfCY mice were aged until tumors were clinically apparent. After sacrificing the mice, tumors were isolated and were washed in sterile PBS twice, minced with sterile scissors and incubated in 2 mg/ml Collagenase Type V (Sigma D4513) in DMEM/F12 at 37^{o}C for 20 minutes, vortexing every 5 minutes. The cells were poured through a 70 um cell strainer into a 50 ml conical tube. Large pieces of tissue trapped in the cell strainer were mechanically dissociated using a syringe plunger. DMEM/F12 was poured through the filter to bring the solution up to 50 ml. The cells were spun down at 2000 rpm for 5 minutes and resuspended in sorting buffer (1X HBSS w/o Ca and Mg with 25 mM HEPES, 5mM $MgCl_2$, 17.5 mM D-glucose, 1X non-essential amino acids [Sigma M7145], 1X glutamax [Life Technologies 35050061], 1 mM sodium pyruvate). Cells were then incubated with rat anti-E-cadherin antibody (ThermoFisher 13-1900) at 1:250 for 15 minutes on ice in the dark. Cells were washed twice with sorting buffer before incubating with APC donkey anti-rat IgG (Jackson Laboratories 712-136-153) at 1:100 and DAPI at 1:1000 for 15 minutes on ice in the dark. Cells were washed twice, resuspended in sorting buffer and transferred to a 5 ml cell strainer-top FACS tube. Tumor cells were gated on DAPI for viability and sorted for YFP^{+}/E-cadherin^{+} epithelial tumor cells and YFP^{+}/E-cadherin^{-} mesenchymal tumor cells. RNA was isolated using the RNeasy Micro Kit (Qiagen 74004) and cDNA was synthesized using the High-Capacity cDNA Reverse Transcription Kit (ThermoFisher 4368813).

TGF-β Treatment *In Vitro*

For *in vitro* induction of EMT, KC cells were treated with recombinant mouse Tgfβ-2 (R&D Systems, 7346-B2-005) at a concentration of 5ng/ml and harvested at the indicated time points. RNA extraction and qPCR was performed as described below.

Cell proliferation assay

A total of 2.0 x 10^3 mouse primary pancreatic cell lines were cultured in 96-well plates and incubated in a humidified atmosphere containing 5% CO_2 at 37°C. Cells were quantified by colorimetric cell p roliferation assay using the WST-1 reagent (Roche, Mannheim, Germany), according to the manufacturer's instructions on indicated days. Absorbance was measured on a microplate reader (Tecan Sunrise, Tecan Group Ltd., Maennedorf, Switzerland) at a wavelength of 450 nm. Each experiment was performed independently in quadruplicate for a total of three experiments. $p<0.05$ was statistically significant (Mann-Whitney-Wilcoxon test). Error bars represent the SEM.

RNAi transfection and Inhibitor treatment

Cells were transfected using Lipofectamine RNAiMAX (Life Technologies) and a final concentration of 5 nM siRNA in Opti-MEM I reduced serum medium (GIBCO, Life Technologies). Mouse Etv1 siRNA was purchased from Dharmacon (Etv1 On-Target Plus Smart Pool (14009), Dharmacon). As control siRNA, On-Target Plus Non-Targeting siRNA Pool (Dharmacon) was used.

MEK inhibition *in vitro*

The MEK-inhibitor U0126 was purchased from Cell Signaling (#9903) and added to the medium of KPfC-cells at a concentration of 10µM for 24h.

Invasion Assay

Invasion assays were performed using BD BioCoat™ Matrigel Invasion Chambers per manufacter's specifications and as described previously.[18] Each experiment was performed in triplicate and $p<0.05$ was statistically significant (Mann-Whitney-Wilcoxon test). Error bars represent the SEM.

Three-dimensional (3D) pancreatic ductal cell organoids

Three-dimensional (3D) pancreatic ductal cell organoids were performed as described previously.[28,29] Assays were performed independently at least three times. $p<0.05$ was statistically significant (Mann-Whitney-Wilcoxon test). For RNA extraction from 3D-cultured cells, collagen coated cells on 4-well-chamber slides (Nunc 177437, Thermo Fisher Scientific) were collected and collagenase digested for 20 minutes at 37℃. After trypsinization, total RNA was extracted with the RNeasy Mini Kit (QIAGEN).

Immunohistochemical/immunofluorescence staining and histopathology

Human TMA construction

Paraffin-embedded samples of primary and metastatic pancreatic cancer tissue from patients who underwent rapid autopsy in association with the Gastrointestinal Cancer Rapid Medical Donation Program were used to

construct a tissue microarray (TMA). The TMA had 16 paired primary pancreatic tumors with matched liver metastasis. There were two samples per primary and metastatic lesion on the TMA in addition to normal controls. All patients died of pancreatic cancer as determined by both gross and histologic analysis. The Johns Hopkins Institutional Review Board approved collection and use of all autopsy and resected tissues for TMA construction. Serial 5 μm sections were made and hematoxylin-eosin (H&E) stained sections were reviewed to ensure the presence of representative lesions in the block. Grading was performed in a blinded fashion by an expert pathologist (CAID). Staining was rated on a scale from 0 to 3 and evaluated for nuclear or cytoplasmic predominance.

Human PanIN TMA construction

PanINs were identified at the time of frozen-section analysis of pancreatic resection specimens from 2007 to 2010 as microscopic papillary or flat noninvasive epithelial neoplasms arising in a pancreatic duct, composed of cuboidal to columnar cells with varying amounts of mucin and degrees of cytologic and architecture atypia as previously described (Kanda M, Matthaei H, Wu J, et al. Presence of Somatic Mutations in Most Early-Stage Pancreatic Intraepithelial Neoplasia. Gastroenterology 2012;142:730–733.e9). PanINs were graded into low grade and high grade lesions based on the degree of cytologic and architectural atypia. The Johns Hopkins Institutional Review Board approved collection and use of tissues for TMA construction. The TMA had17 low-grade PanIN and 5 high-grade PanIN lesions suitable for interpretation in addition to normal controls. Serial 5 μm sections were made

and hematoxylin-eosin (H&E) stained sections were reviewed to ensure the presence of representative lesions in the block. Grading was performed in a blinded fashion. Staining was rated on a scale from 0 to 3 and evaluated for nuclear or cytoplasmic predominance.

Human PDAC immunohistochemistry

Human PDAC samples (n=7) from patients who underwent operative resection for their pancreatic cancer were obtained from the University of Pennsylvania Molecular Pathology and Imaging Core Facility (MPIC). Serial 5 µm sections were made and hematoxylin-eosin (H&E) stained sections were reviewed to ensure the presence of representative lesions in the block. The lesions were examined carefully and three representative areas that contained predominantly (>80%) tumor and three representative areas that contained predominantly (>80%) stroma were evaluated. Subsequently, grading was performed, rating on a scale from 0 to 3 and evaluated for nuclear or cytoplasmic predominance. Averages for each patient for tumor predominant staining and stroma predominant staining were then calculated.

Mouse Immunohistochemistry and Immunofluorescence

Tissue was fixed in zinc formalin overnight, transferred to 70% ethanol and submitted to the University of Pennsylvania Molecular Pathology and Imaging Core where paraffin-embedded sections were cut for hematoxylin and eosin (H&E) staining, IHC/IF, and trichrome staining.

In brief, antigen retrieval was performed using citric acid buffer (pH 6.0) and pressure cooking. Sections were washed with PBS and blocked using TBS + 0.3% Triton-X (TBS-T) with 5% normal donkey serum (Jackson ImmunoResearch) for 1 h at room temperature. Primary antibodies were applied and incubated overnight at 4℃. After two w ashes with TBS-Tween, secondary antibodies were applied and incubated for 30 min at 37℃. DAPI counterstaining was performed (Sigma-Aldrich).

The following primary antibodies were used: anti-Etv1(1:250; Abcam ab81086), anti-GFP (1:250; Abcam ab13970), anti-SPARC(1:50; R&D Systems AF942), anti-ECAD(1:500; BD Biosciences #610182), anti-ECAD(1:1000; R&D Systems mAb7481), anti-RFP(1:200; Abcam ab34771), anti-SMA(1:7000; Sigma A5228), anti-LOX(1:250; Novus NB1002527), anti-Collagen I(1:250; Southern Biotech 1310-01), GFAP (courtesy of Dr. Noga Vardi at University of Pennsylvania; 1:50), and Ki67 (1:1000; Novocastra #301119)

Terminal deoxynucleotidyl transferase–mediated deoxyuridine triphosphate nick-end labeling (TUNEL) assays were performed using the in situ cell death detection kit (Roche, Mannheim, Germany).

Hyaluronic Acid was assessed utilizing the specific molecular probe for hyaluronic acid, HTI601. Staining was performed in a completely blinded fashion by Halozyme (San Diego, CA).

Semiquantitative grading was performed utilizing semi-automated ImageJ software analysis with the same threshold for each stain; results were expressed as percentage staining per visual field (trichrome, hyaluronic acid, SMA, Collagen I). In instances where automated image analysis was unable to be performed, manual counting utilizing ImageJ was performed for SPARC staining (expressed as a ratio of delaminated cancer cells co-expressing YFP and SPARC per DAPI positive nuclei), LOX staining (LOX positive cells per DAPI positive nuclei), and GFAP staining (GFAP positive cells per high power field). A minimum of 4 animals per group and at least 5 different high power fields per animal were examined for quantification. Ki67 and TUNEL assay were graded as positive cells per high power field with 10 high power fields examined in 3 animals per group. $p<0.05$ was statistically significant (Fischer's Exact Test). Error bars represent the SEM.

Quantitative RT-PCR

RNA was isolated utilizing RNeasy Mini Kit (QIAGEN). 1µg of RNA was transcribed into cDNA (Taqman Reverse Transcription Reagents) and assayed utilizing quantitative real-time PCR with Power SYBR Master Mix (Applied Biosystems) on the StepOnePlus System (Applied Biosystems). Primers are listed in Supplemental Table 1. $p<0.05$ was statistically significant (Mann-Whitney-Wilcoxon test). Error bars represent the standard deviation (SD).

Western blotting

Western blotting was performed as described previously.[18] Anti-FLAGM2 antibody (1:1000, F1804, Sigma Aldrich) and anti-mouse β-actin (1:5000, A5316, Sigma-Aldrich) antibody were used for detection. Experiments were performed in triplicate.

Luciferase assay and site directed mutagenesis

Luciferase reporter assays were performed using a Luciferase Assay Kit (Promega).[30] In brief, KPfC control or KPfC mEtv1 cells were plated onto 6-well plates at a density of $1.3x10^5$ cells per well. A total of 500 ng of pGL3-basic (Promega), pGL3-Sparc-Promoter (-307bp to +150bp), or pGL3-Has2-Promoter (-1186bp to +87bp) (Supplemental Table 1) were co-transfected with KPfC control and KPfC mEtv1 cells. Forty-eight hours post transfection cells were lysed in 200 mL of passive lysis buffer and assayed for luciferase activity using the Luciferase Assay Kit (Promega, Madison, WI).

A mutant promoter construct of Has2 was generated using a forward primer containing mutant nucleotides spanning region -1129bp to -1109bp (Etv1 binding site) (Supplemental Table 1, Supplemental Figure 5B). Successful mutation of the Etv1 binding site was confirmed by sequencing.

Orthotopic Transplant Procedures

The tumor volume was measured with digital calipers using the following formula: π/6 x (L x W x W), where L is the tumor at its longest and W is at its shortest.[32] Ascites was graded at the time of sacrifice by two independent observers into the following grades: 1 - loculated perihepatic ascites, 2 –

localized abdominal ascites, 3 – free-flowing abdominal ascites upon incision. Liver sections were collected and mounted onto glass slides at the maximal footprint and then four additional sections, each 300µm apart, were collected. Metastatic foci were identified on H&E, photographed and adjudicated independently by 2 blinded reviewers. Metastases were then counted for cell number and measured utilizing digital calipers on ImageJ. Metastases were classified into three subtypes based on previous literature[33,34]: isolated tumor cells (ITC) that were <0.2mm and <200cells, micrometastasis that were 0.2-2mm in size with >200cells, or macrometastasis that were >2mm in size. Lung metastases were examined with a single slide at maximal footprint. Metastases were confirmed utilizing immunofluorescence staining for YFP or dTomato.

SUPPLEMENTAL FIGURE 1

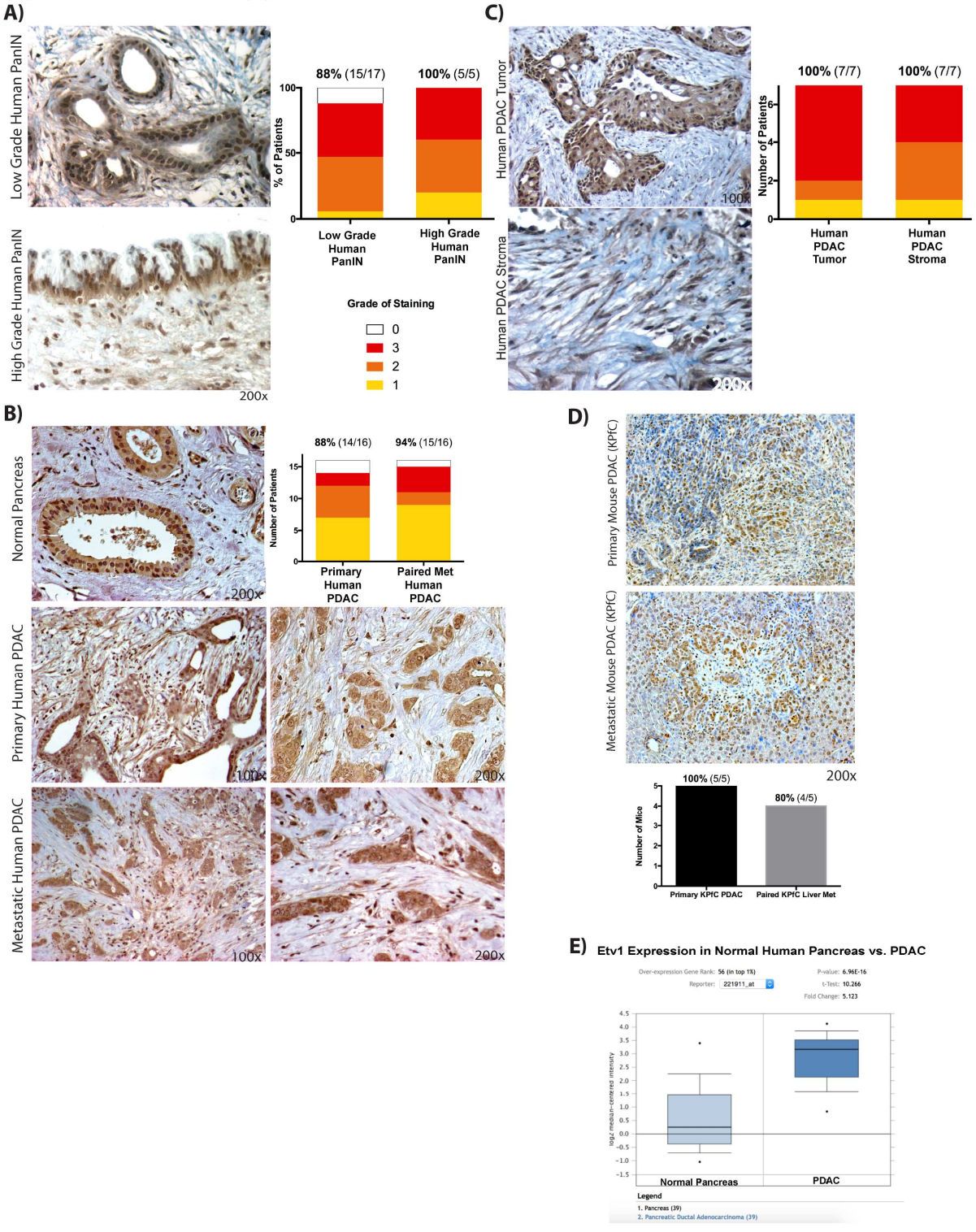

E) **Etv1 Expression in Normal Human Pancreas vs. PDAC**

SUPPLEMENTAL FIGURE 2

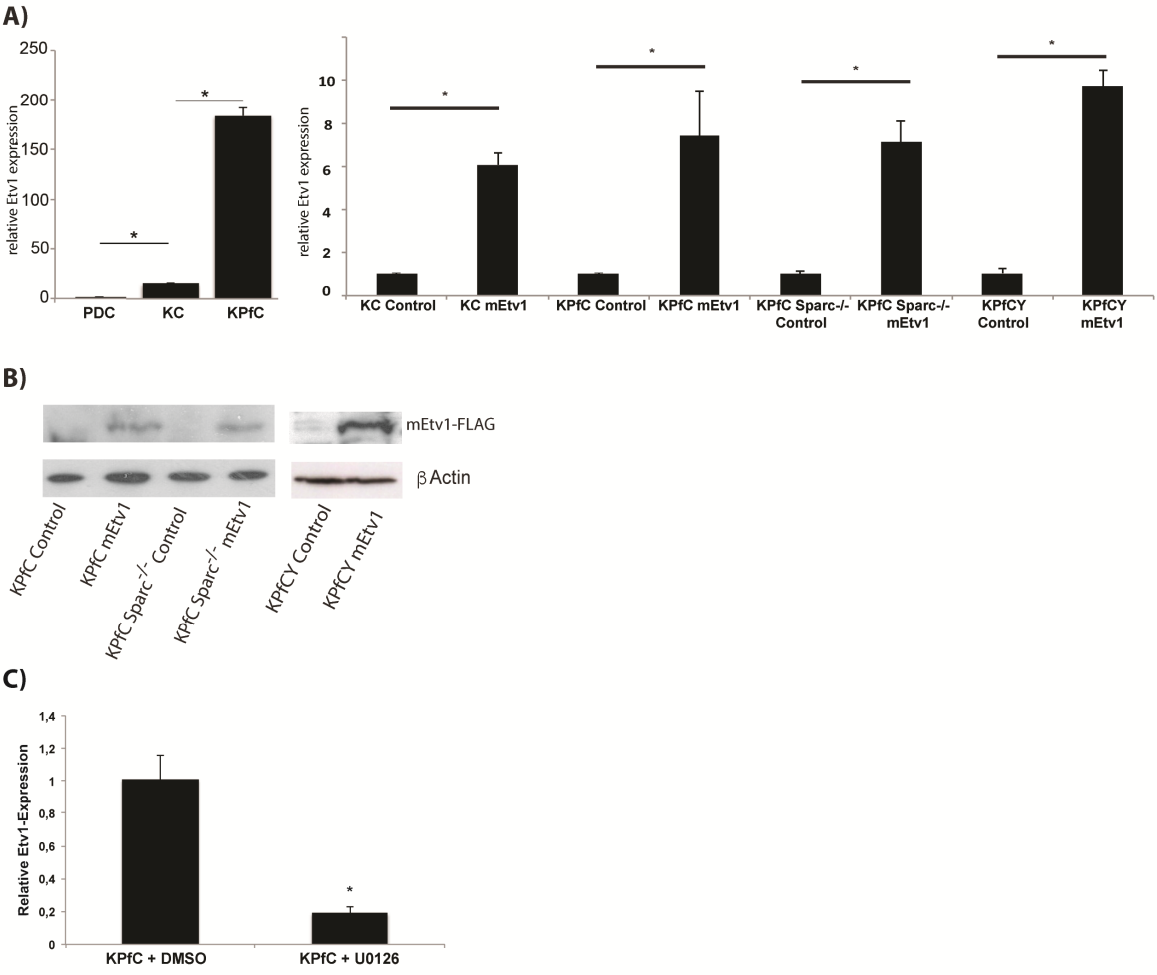

SUPPLEMENTAL FIGURE 3

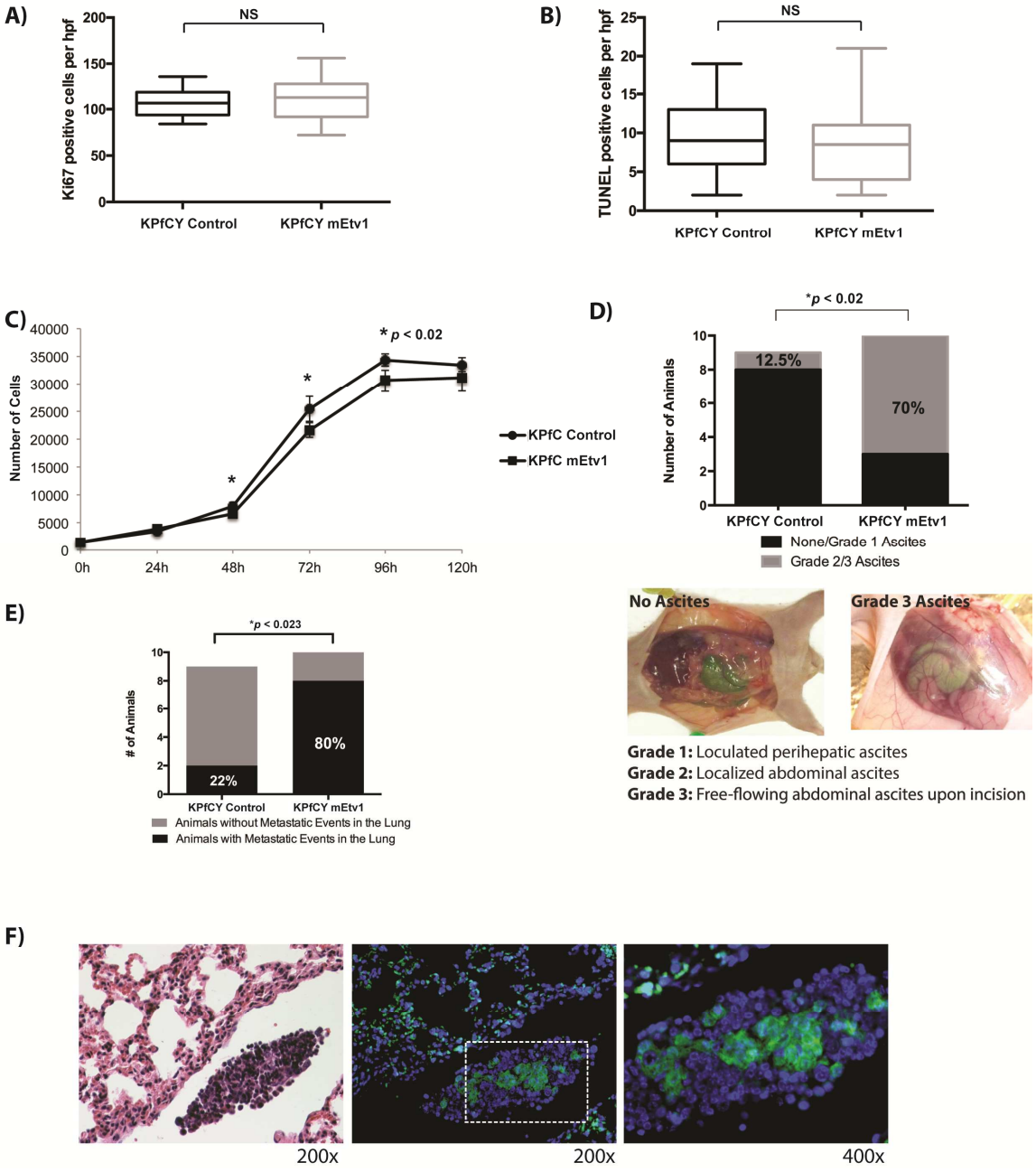

SUPPLEMENTAL FIGURE 4

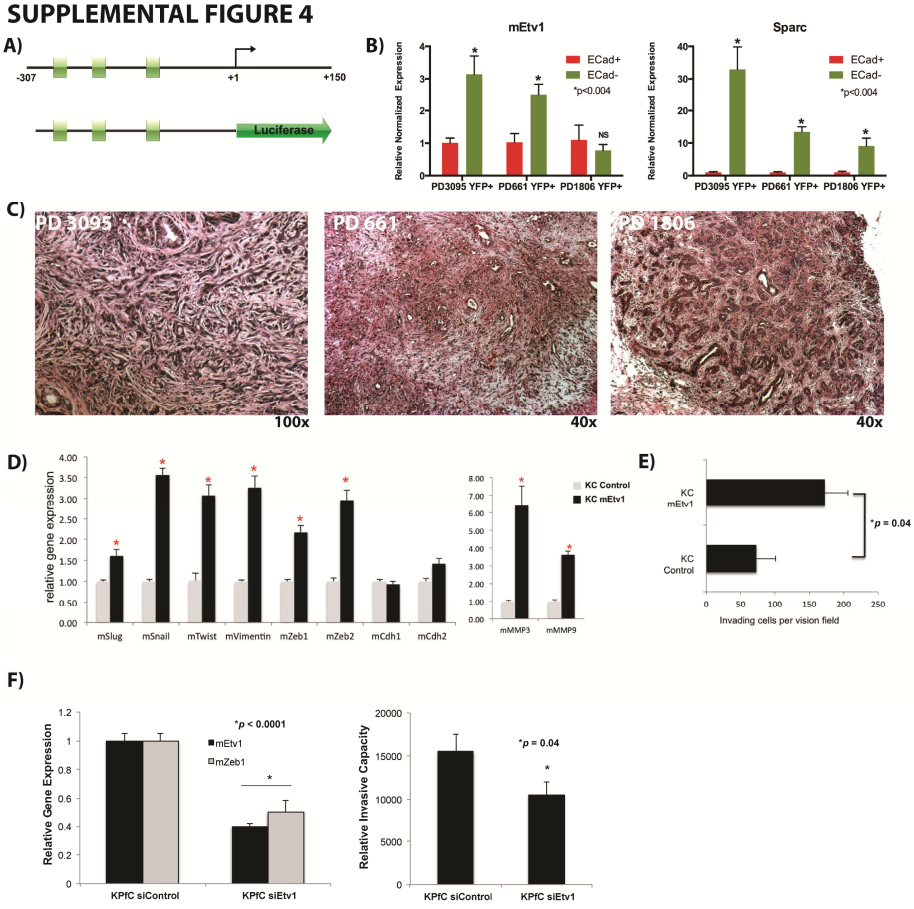

SUPPLEMENTAL FIGURE 5

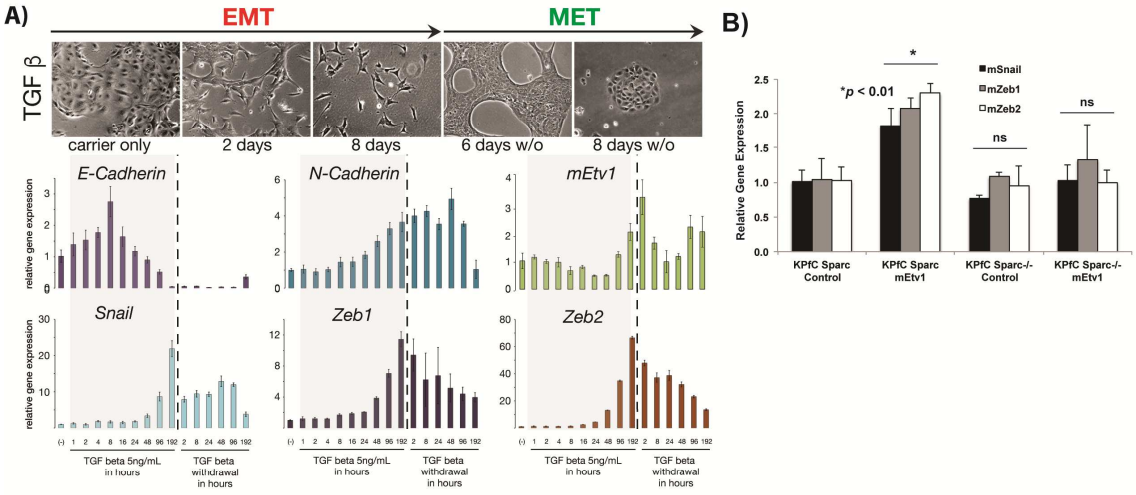

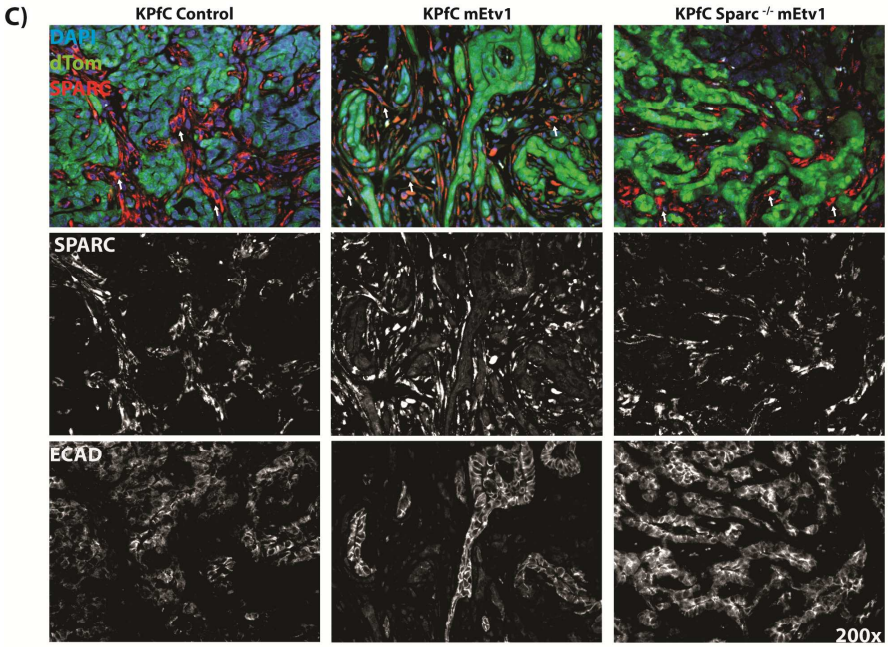

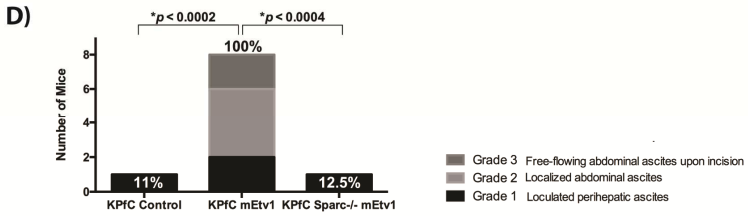

SUPPLEMENTAL FIGURE 6

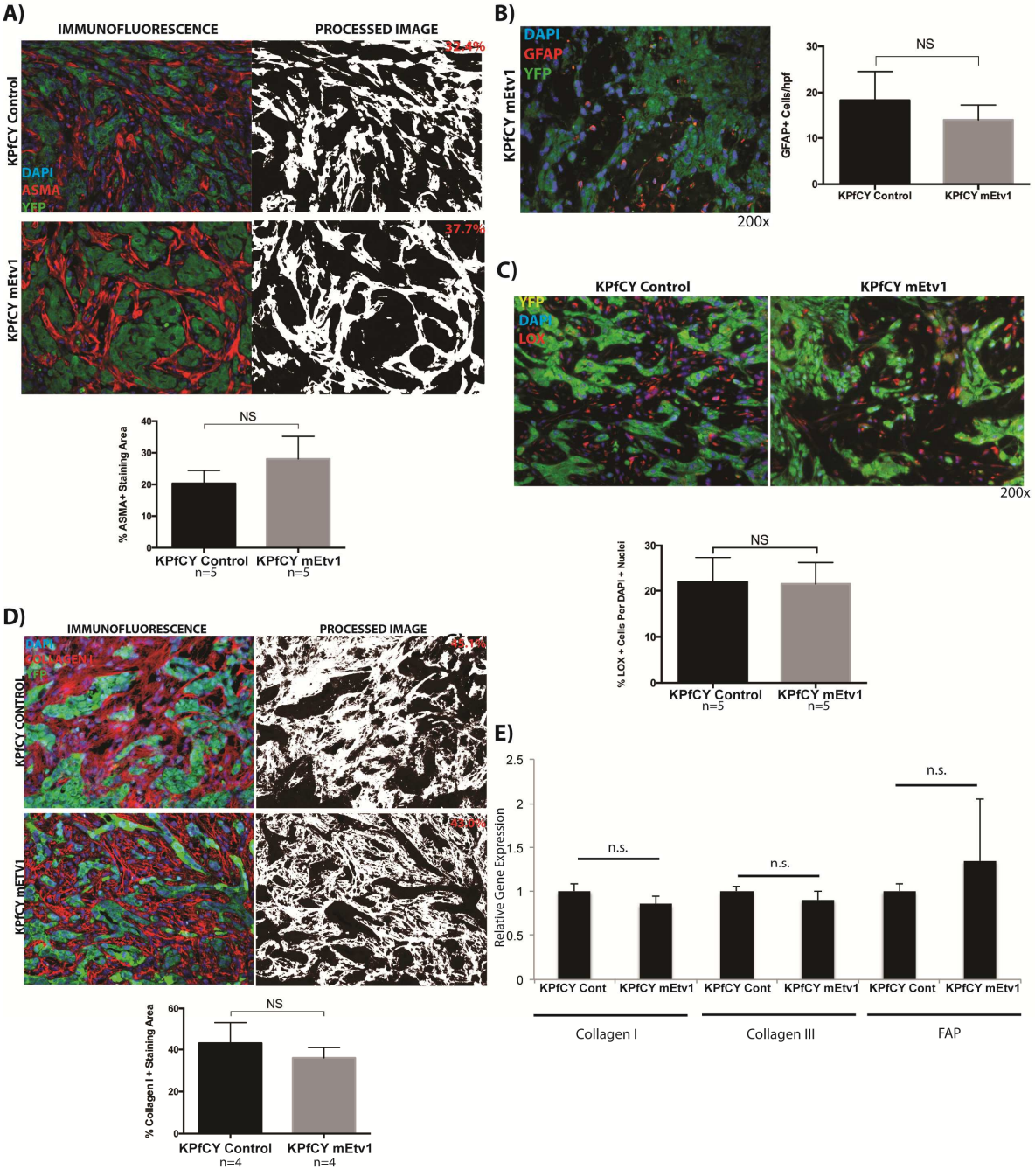

SUPPLEMENTAL FIGURE 7

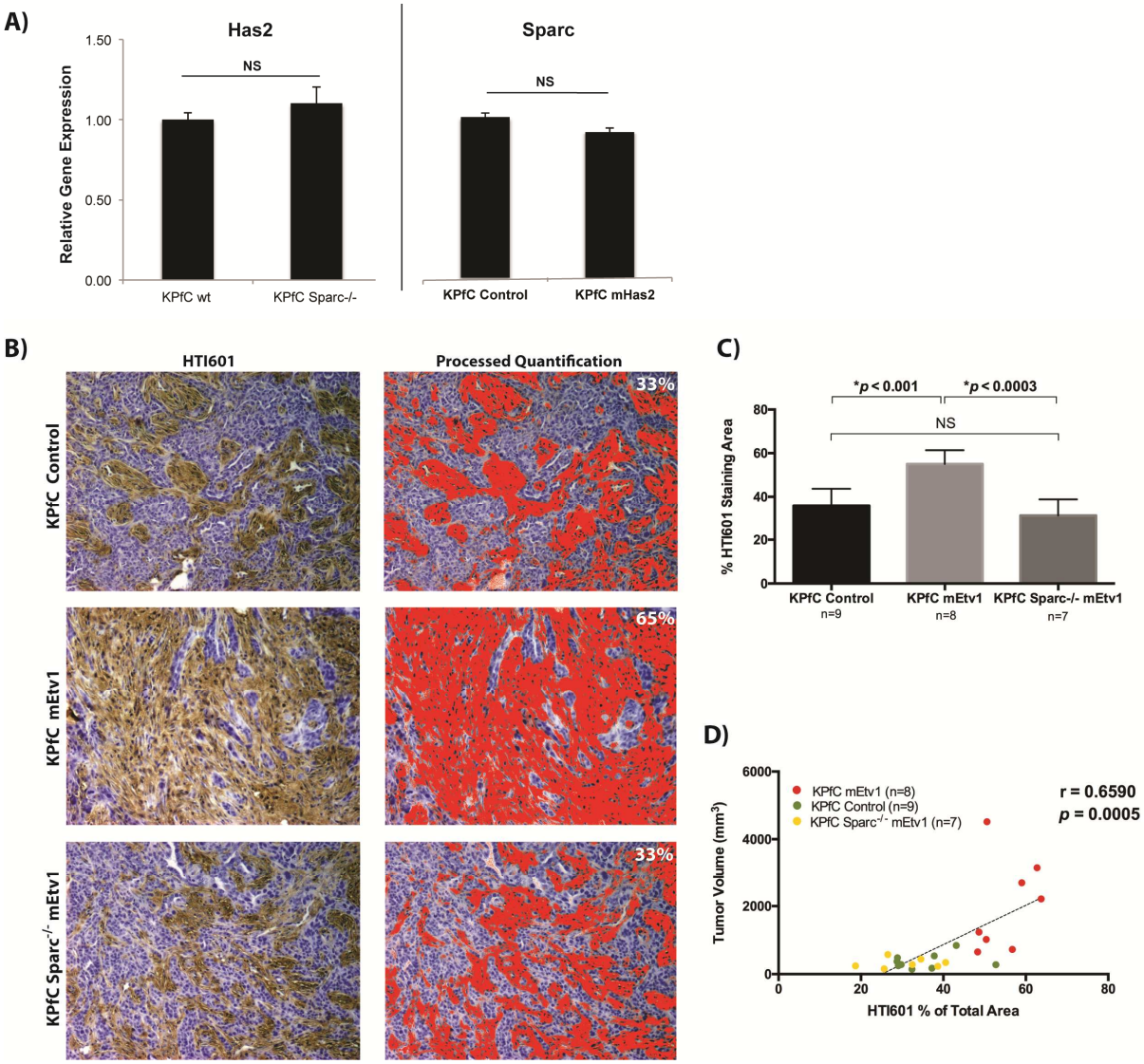

Supplemental Table 2: Predicted Ets-binding sites in ECM components of PDAC

Gene	Gene Symbol	Accession Number	Number of predicted Ets binding sites
Biglycan	Bgn	GXP_258545	10
Decorin	Dcn	GXP_41011	3
Fap-α	Fap	GXP_149503	9
Fibronectin	Fn1	GXP_223655	9
Has 1	Has1	GXP_111427	2
Has 2	Has2	GXP_307656	5
Has 3	Has3	GXP_142264	10
Lumican	Lum	GXP_41177	5
Mmp 2	Mmp2	GXP_155151	8
Mmp 9	Mmp 9	GXP_203704	8
Mmp11	Mmp11	GXP_2522592	4
Periostin	Postn	GXP_308962	4
Sparc/Osteonectin	Sparc	GXP_231199	3
Tenascin C	Tnc	GXP_431890	8
Thrombospondin 1	Thbs1	GXP_287201	3
Thrombospondin 2	Thbs2	GXP_111403	6
Timp-1	Timp1	GXP_897141	6
Timp-2	Timp2	GXP_252148	5
tPA	Plat	GXP_270591	4
uPA	Plau	GXP_125020	6
Versican	Vcan	GXP_168864	6
Vitronectin	Vtn	GXP_3065104	5